527073

Department of Molecular Biology, Scripps Research Institute, La Jolla, California, 92037, USA.
Cell (UNITED STATES) Mar 22 1996, 84 (6) p863-74, ISSN 0092-8674 Journal Code: 0413066

NPL ✓ Adonis ✓
MIC BioTech MAIN
NO Vol NO NOS
Ck Cite Dupl Request
Call #

7) $$$ 13135380 PMID: 8805536
Crystal structure of the yeast cell-cycle control protein, p13suc1, in a strand-exchanged dimer.
Khazanovich N; Bateman K; Chernaia M; Michalak M; James M
Medical Research Council Group in Protein Structure and Function, University of Alberta, Edmonton, Alberta, Canada T6G 2H7.
Structure (London, England) (ENGLAND) Mar 15 1996, 4 (3) p299-309, ISSN 0969-2126 Journal Code: 9418985

8) *** Crystal structure and mutational analysis of the Saccharomyces cerevisiae cell cycle regulatory protein Cks1: implications for domain swapping, anion binding and protein interactions.
Bourne Y; Watson M H; Arvai A S; Bernstein S L; Reed S I; Tainer J A
Centre National de la Recherche Scientifique, Marseille, France. yves@afmb.cnrs-mrs.fr
Structure with Folding & design (ENGLAND) Aug 15 2000, 8 (8) p841-50, ISSN 0969-2126 Journal Code: 100889329
Document type: Journal Article

Thank you.
MINH TAM DAVIS
ART UNIT 1642, ROOM 3A24, MB 3C18
272-0830

10/057,813
1/31/05

Crystal structure of the yeast cell-cycle control protein, p13^{suc1}, in a strand-exchanged dimer

N Khazanovich[1†], KS Bateman[1†], M Chernaia[1], M Michalak[2] and MNG James[1*]

Background: p13^{suc1} from fission yeast is a member of the CDC28 *k*inase *s*pecific (CKS) class of cell-cycle control proteins, that includes CKS1 from budding yeast and the human homologues CksHs1 and CksHs2. p13^{suc1} participates in the regulation of p34^{cdc2}, a cyclin-dependent kinase controlling the G_1–S and the G_2–M transitions of the cell cycle. The CKS proteins are believed to exert their regulatory activity by binding to the kinase, in which case their function may be governed by their conformation or oligomerization state. Previously determined X-ray structures of p13^{suc1}, CksHs1 and CksHs2 show that these proteins share a common fold but adopt different oligomeric states. Monomeric forms of p13^{suc1} and CksHs1 have been solved. In addition, CksHs2 and p13^{suc1} have been observed by X-ray crystallography in assemblies of strand-exchanged dimers. Analysis of various assemblies of the CKS proteins, as found in different crystal forms, should help to clarify their role in cell-cycle control.

Results: We report the X-ray crystal structure of p13^{suc1} to 1.95 Å resolution in space group $C222_1$. It is present in the crystals as a strand-exchanged dimer. The overall monomeric fold is preserved in each lobe of the dimer but a single β-strand (Ile94–Asp102) is exchanged between the central β-sheets of each molecule.

Conclusions: Strand exchange, which has been observed for p13^{suc1} in two different space groups, and for CksHs2, is now confirmed to be an intrinsic feature of the CKS family. A switch between levels of assembly may serve to coordinate the function of the CKS proteins in cell-cycle control.

Addresses: [1]Medical Research Council Group in Protein Structure and Function and [2]Cardiovascular Disease Research Group, Department of Biochemistry, University of Alberta, Edmonton, Alberta, Canada T6G 2H7.

†NK and KSB contributed equally to this work.

*Corresponding author.

Key words: cell cycle, domain swapping, p13^{suc1}, strand-exchanged dimer, X-ray structure

Received: **4 Dec 1995**
Revisions requested: **22 Dec 1995**
Revisions received: **15 Jan 1996**
Accepted: **31 Jan 1996**

Structure 15 March 1996, 4:299–309

Introduction

p13^{suc1} from fission yeast (*Schizosaccharomyces pombe*) is essential for cell viability [1–4] and is a member of the *C*DC28 *k*inase *s*pecific (CKS) class of cell-cycle control proteins. This 13 kDa protein binds to p34^{cdc2} [5], a cyclin-dependent kinase fundamental to the G_2–M and G_1–S phase transitions of the cell cycle [6–8]. Throughout the cell cycle, levels of the kinase remain constant [9] so that the intricate regulation of its activity depends on the actions of other proteins such as cyclins, phosphatases, kinases and p13^{suc1} [10,11]. The interaction between p13^{suc1} and p34^{cdc2} was first noticed when a temperature-sensitive mutant of p34^{cdc2} kinase was rescued by the overexpression of p13^{suc1} [1,12]. A similar result was obtained for CKS1 and a temperature-sensitive mutant of CDC28, the *Saccharomyces cerevisiae* homologues of p13^{suc1} and p34^{cdc2}, respectively [13]. This interaction may apply to a wide range of species, as homologues of both p13^{suc1} and p34^{cdc2} kinase have been found in plants [14] and other eukaryotes [15,16].

In other studies, p13^{suc1} has been proposed to inhibit p34^{cdc2} kinase [3,17,18]. Overexpression of p13^{suc1} resulted in a delayed entry into mitosis [1]. It was suggested that p13^{suc1} prevented the dephosphorylation of Thr14 or Tyr15 on p34^{cdc2} required for kinase activation [17]. The exact mode of action of p13^{suc1} is not currently understood. This protein is not a substrate for the kinase [5], and does not appear to possess any catalytic activity. p13^{suc1} probably functions by binding to the cyclin-dependent kinase (CDK). In this case, regulation may involve changes in conformation or oligomerization of p13^{suc1}. In order to elucidate the mechanism by which p13^{suc1} regulates p34^{cdc2} kinase, it is useful to examine the various assemblies of p13^{suc1} and its homologues that have been found in different crystal forms.

The crystal structure of p13^{suc1} originally revealed a monomeric form of the molecule [19]. Structures of the two p13^{suc1} homologues from humans, CksHs1 and CksHs2, have also been determined [20,21]. The overall fold of the proteins from *S. pombe* and from humans is very similar. However, different levels of assembly were observed for the human isoforms. CksHs1 is a monomer, while CksHs2 forms a hexamer consisting of three dimers. In the monomeric structures of p13^{suc1} and CksHs1, the C-terminal β-strand participates in a four-stranded β-sheet (Fig. 1a). In the CksHs2 dimer, each monomer contributes its C-terminal β-strand to the four-stranded β-sheet in the adjacent monomer, forming a tight dimer association.

Figure 1

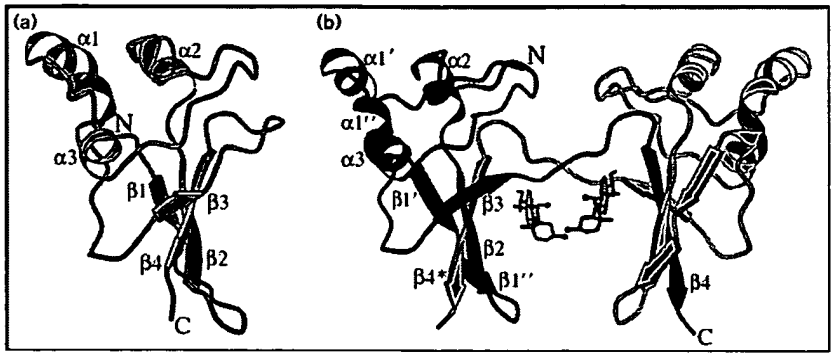

The two forms of p13^{suc1}. **(a)** The monomer of p13^{suc1}, observed in the hexagonal space group (p13hex) [19]. **(b)** The strand-exchanged dimer of p13^{suc1} (p13or). Two symmetry-related CHAPS molecules are present in the arch of the dimer. Labelling of secondary structure of p13or corresponds to that shown in Figure 3. The first α-helix has been designated as two helical segments, α1′ and α1″, separated by a kink at Pro20. The first β-strand is also divided into β1′ and β1″ by a β-bulge at Pro29. Strand β4* originates from the strand-exchange partner. (Figure generated using MOLSCRIPT [37].)

Recently, a strand-exchanged dimer of p13^{suc1}, similar to the one found for CksHs2, has been observed in space group $P2_12_12_1$ [22]. We report the crystal structure of p13^{suc1}, also in a strand-exchanged dimer, in space group $C222_1$ (Fig. 1b). The new p13^{suc1} structure extends the idea that oligomerization controls the function of p13^{suc1} and its homologues, and demonstrates that the unusual strand-exchange interaction is common to this family of cell-cycle control proteins.

Results and discussion

The p13^{suc1} strand-exchanged dimer

The structure of p13^{suc1} has been solved in the orthorhombic space group $C222_1$ (p13or) and has been found to form a strand-exchanged dimer (Figs 1b,2). The protein studied here was recombinant p13^{suc1}, which contained residues Ser2–Lys106. The N-terminal methionine and seven C-terminal residues have probably been removed during expression by aminopeptidase and tryptic cleavages, respectively. The final model includes residues, Ser2–Asp102, 72 water molecules and a portion of the detergent 3-[(3-cholamidopropyl)dimethylammonio]-1-propanesulfonate hydrate (CHAPS) (Fig. 1b). Residues 103–106 are not defined in the electron-density map, and are believed to be highly disordered in the crystal. The R-factor is 18.7% for 8500 reflections (Table 1). The model has good stereochemistry, and all residues fall within the allowed regions of the Ramachandran plot [23]. p13^{suc1} has been solved previously in a hexagonal space group (p13hex) where it was found as a discrete monomer [19]. The p13hex monomer consists of a four-stranded antiparallel β-sheet flanked on one edge by three helices forming a wedge-shaped molecule (Fig. 1a). The fold of each lobe of the strand-exchanged dimer is essentially the same as that of the p13^{suc1} monomer (Table 2); however, in the p13or dimer, a crystallographic twofold symmetry-related molecule contributes strand β4 to the four-stranded β-sheet (Fig. 1b). The segment of polypeptide connecting β3 to β4 adopts an extended conformation in the dimer, but forms a loop in the monomer.

Comparison of p13or with the CksHs2 strand-exchanged dimer

The strand-exchange interaction has been observed for another member of the CKS family, the human homologue CksHs2. CksHs2 is shorter than p13^{suc1}, missing 19 residues at the N terminus, six at the C terminus, and a 9-residue loop from Phe56–Arg64 (Fig. 3). It is interesting to compare the nature of strand exchange observed for p13^{suc1} and CksHs2. The cross-over occurs at the same location in the sequence, where a significant number of conserved residues are found (Fig. 3), but there are notable structural differences between the strand-exchange regions of the two proteins.

The p13^{suc1} and CksHs2 dimers contain a crystallographic twofold symmetry axis at the centre of the strand-exchange region (Fig. 4a,b). The axis is found between His88 and His88′ in p13^{suc1}, and between Glu63 and Glu63′ in CksHs2. In the sequence alignment, however, Glu63 of CksHs2 corresponds to Glu91 of p13^{suc1}, which is three residues away from His88 (Fig. 3). As a result, different residues are juxtaposed within the two strand-exchange regions, placing the lobes of the p13^{suc1} dimer closer together than those of CksHs2. For instance, the Cα atoms of Tyr85 and Tyr85′ in p13^{suc1} are 22 Å apart, whereas Tyr57 and Tyr57′ in the C subunits of CksHs2 are separated by 38 Å, demonstrating that the strand-exchange region in p13^{suc1} is more compact than in CksHs2.

In addition, the p13^{suc1} polypeptide chain changes direction at Tyr85 and bends at Pro92, such that the two exchanging strands of p13^{suc1} point in different directions with respect to the strands of CksHs2 (Fig. 5a). As a result, the p13or dimer is significantly bent in comparison with the CksHs2 dimer. The bending is probably caused by the nine-residue insertion (56–64) in p13^{suc1} relative to the CksHs2 sequence (Fig. 3). These nine residues increase the size of the loop connecting α2 and α3 in p13^{suc1}. The possibility of a sterically unfavourable interaction with residues in this loop may prevent the exchanged strand, β4,

Figure 2

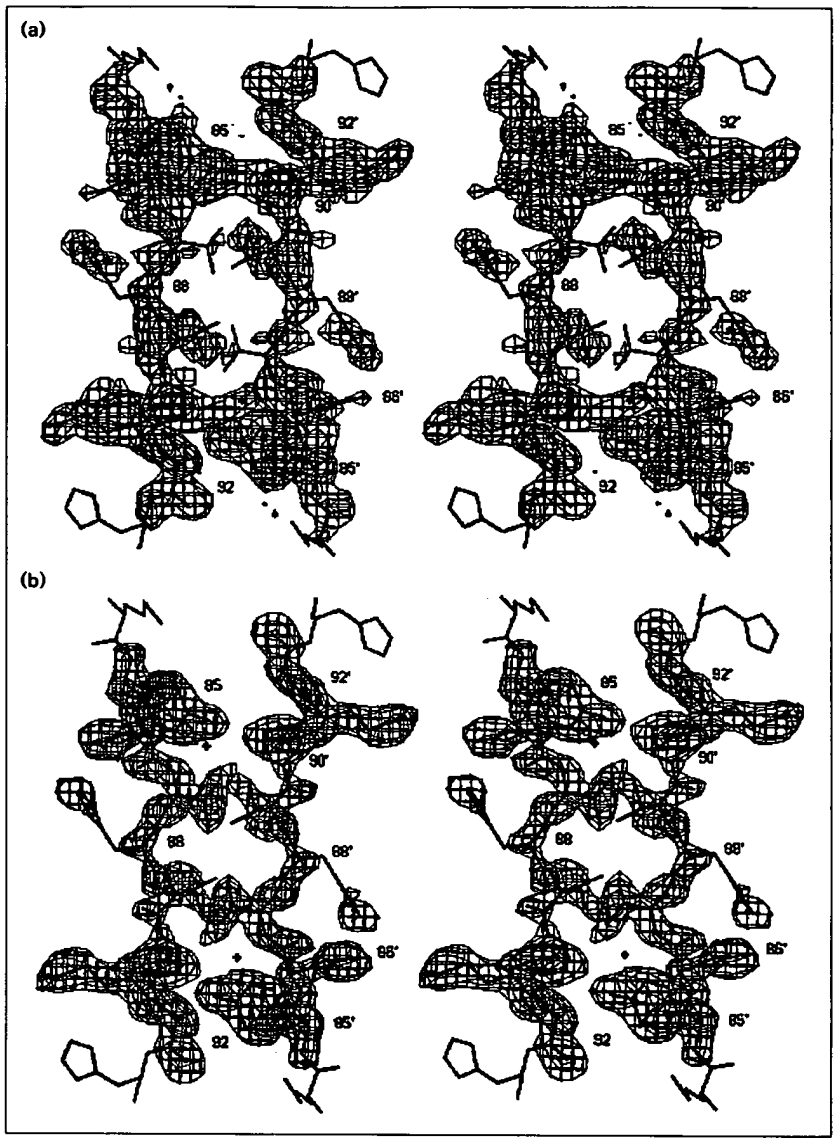

Electron density of the strand-exchange region. **(a)** Electron density with phases derived from the molecular replacement model (p13hex), initially refined with X-PLOR [32]. The phasing model included a loop connecting β3 to β4, rather than an exchanged strand. Residues Tyr85–Pro92 of the final refined model are shown ($2F_o$–F_c density, contoured at 1σ). **(b)** Electron density with phases derived from the final refined model (p13or) omitting residues 85–92. A water molecule in this region (represented by +) was not omitted. The final refined model is shown, residues Tyr85–Pro92 (F_o–F_c density, contoured at 2σ).

from following the same direction as the equivalent strand in CksHs2. In a superposition of CksHs2 with p13or, the Cγ2 atom of Ile59 from the CksHs2 strand is only 2.4 Å away from Thr62 in the p13or loop. The position corresponding to Ile59 in CksHs2 is occupied by Val87 in p13^{suc1}. This β-branched residue would presumably make a similar close contact with the α2–α3 loop if the p13^{suc1} strand followed the same path as in CksHs2. The kink at Pro90 also appears to be required to avoid a steric collision.

With the exception of the two sites of difference, Tyr85 and Pro92, the exchanged strands of both proteins adopt similar extended conformations, as judged by their main-chain dihedral angles (Table 3). The exchanged strands are also stabilized in a similar manner in both dimers (Fig. 4a,b). At the centre of the p13or cross-over region, Val87 Cγ of one monomer interacts with Val89′ Cγ of the symmetry-related monomer. Within each strand there are two salt bridges: between Glu86 and His88, and between Glu91 and His93 (Fig. 4a). In CksHs2, the aliphatic portion of the Glu63 side chain (Cβ, Cγ) appears to make a hydrophobic contact with the side chain of Glu63′ from the strand in the other monomer. His60 participates in electrostatic interactions with Glu61 and Glu63 in the same strand. In neither case are β-sheet main-chain hydrogen bonds found between the exchanging strands. Although the exchanging strands run in antiparallel directions in both dimers, in p13or they are skewed (Fig. 4a).

Table 1

Data collection and refinement statistics.

Data collection	
resolution range (Å)	50–1.95
number of crystals used	1
number of observations	53 600
number of unique reflections	9859
Completeness of data (%)	
all data	97.5
1.98–1.95 Å	81.4
F>1σ	96.8
R_{merge} (%)	4.88
Final refinement parameters	
resolution range (Å)	6.0–1.95
number of protein atoms	848
number of solvent atoms	72
number of detergent atoms	26
R-factor (%)	18.7
Free R-factor (%)	24.1
Rms deviations from ideal geometry for the protein	
bond lengths (Å)	0.006
bond angles (°)	1.422
planar groups (°)	0.017
Average B-factors (Å²)	
main-chain	20.8
side-chains	27.0
solvent	41.5
CHAPS	32.8 (occupancy=0.67)

Space group: $C222_1$. Unit cell dimensions: a=43.27 Å, b=55.28 Å, c=111.80 Å. V_m=2.7 Å³ Da^{-1}, one molecule per asymmetric unit.

Table 2

Rms deviations for superposition of p13or, p13hex and CksHs2 in the common regions.

	p13or	p13hex(A)	p13hex(B)	CksHs2(C)
p13or	–	0.71	0.58	0.81
p13hex(A)	348(mc)*	–	0.43	0.83
p13hex(B)	348(mc)*	384(mc)†	–	0.70
CksHs2(C)	52(Cα)‡	52(Cα)‡	52(Cα)‡	–

Superpositions were calculated with the program O [33]. Values above the diagonal are rms deviations (in Å). Below the diagonal, the number of atoms used in the superposition is given with the atom type in parentheses (mc=main chain; Cα=α-carbon). *Residues 8–85, 93–101 (p13hex) versus 8–85, 93′–101′ (p13or). †Residues 6–101. ‡Residues 5–26, 37–57, 65′–73′ (CksHs2) versus 24–45, 65–85, 93′–101′ (p13or).

Despite the different overall shapes of the p13or and CksHs2 strand-exchanged dimers, their domains superimpose well (Table 2). The shape disparity probably stems from the need to accommodate a longer α2–α3 loop in $p13^{suc1}$. The loop enforces a bend and a twist in the strand-exchange region, which decreases the distance between the lobes of the $p13^{suc1}$ dimer relative to CksHs2. In the CksHs2 structure, three strand-exchanged dimers are assembled into a hexamer [21]. Because the $p13^{suc1}$ dimer is bent with respect to CksHs2, further assembly into a similar hexamer does not appear possible. The human and *S. pombe* homologues may thus involve different multimeric states for activity.

Comparison of p13or with the previously determined $p13^{suc1}$ strand-exchanged dimer

The strand-exchanged dimer of $p13^{suc1}$ has now been observed in two space groups: $P2_12_12_1$ with two dimers in the asymmetric unit [22] and $C222_1$. A comparison of the three dimers is shown in Figure 5b. A superposition of one monomer from each of the three dimers orients its strand-exchanged partner such that a twist becomes evident. The most striking feature in the comparison of p13or with the previously described strand-exchanged dimers is that p13or exhibits a twist which is of intermediate severity relative to the $P2_12_12_1$ dimers [22]. In effect, this set of structures defines a motion in the strand-exchanged dimer.

A comparison of the main-chain dihedral angles shows that the conformations of the residues in this region do not differ significantly among the three independently

Figure 3

```
                          10        20        30        40        50        60
                          ←α1′→ ←α1″→←β1′→ ←β1″→  ←— β2 —→  ←—α2—→
S.pombe p13suc1       MSKSGVPRLLTASERERLEPFIDQIHYSPRYADDEYEYRHVMLPKAMLKAIPTDYFNPETGTLR
S.cerevisiae CKS1  MYHHYHAFQGRKLTDQERARVLEFQDSIHYSPRYSDDNYEYRHVMLPKAMLKVIPSDYFNSEVGTLR
Human CksHs2                          MAHKQIYYSDKYFDEHYEYRHVMLPRELSKQYPKTH
Human CksHs1                          MSHKQIYYSDKYDDEEFEYRHVMLPKDIAKLVPKTH
P.vulgata CKS1                        MSARQIYYSDKYFDEDFEYRHVMLPKDIAKMVPKNH

                          70        80        90        100       110
                          ←—α3—→          ←β3→      ←—β4—→
S.pombe p13suc1       ILQEEEWRGLGITQSLGWEMYEVRVPEPHILLFKREKDYQMKFSQQRGG
S.cerevisiae CKS1     KLTEDEWRGLGITQSLGWEHYECHAPEPHILLFKRPLNYEAELRAATAAAQ,HQTQSISNDMQVPPQIS
Human CksHs2          LMSEEEWRRLGVQQSLGWVHYMIHEPEPHILLFRRPLPKDQQK
Human CksHs1          LMSESEWRNLGVQQSQGWVHYMIHEPEPHILLFRRPLPKKPKK
P.vulgata CKS1        LMSEAEWRSIGVQQSHGWIHYMKHEPEPHILLFRRKVTGQ
```

Sequence alignment of $p13^{suc1}$ from *S. pombe* and its homologues, CKS1 from *S. cerevisiae*, human CksHs1 and CksHs2, and CKS1 from *Patella vulgata* [16]. $p13^{suc1}$ numbering and secondary structure elements of p13or are indicated above the sequence. (α1′ and α2 are 3_{10}-helices.) The residues involved in strand exchange in $p13^{suc1}$ and in CksHs2 are shown bold. Boxes indicate conserved residues. Q_{16} in the *S. cerevisiae* CKS1 sequence indicates a run of 16 glutamine residues.

Figure 4

The strand-exchange regions of p13or and CksHs2. **(a)** p13or, residues 83–93. **(b)** CksHs2, subunits C, residues 57–69. In both cases, primed numbers indicate residues of the symmetry-related strand.

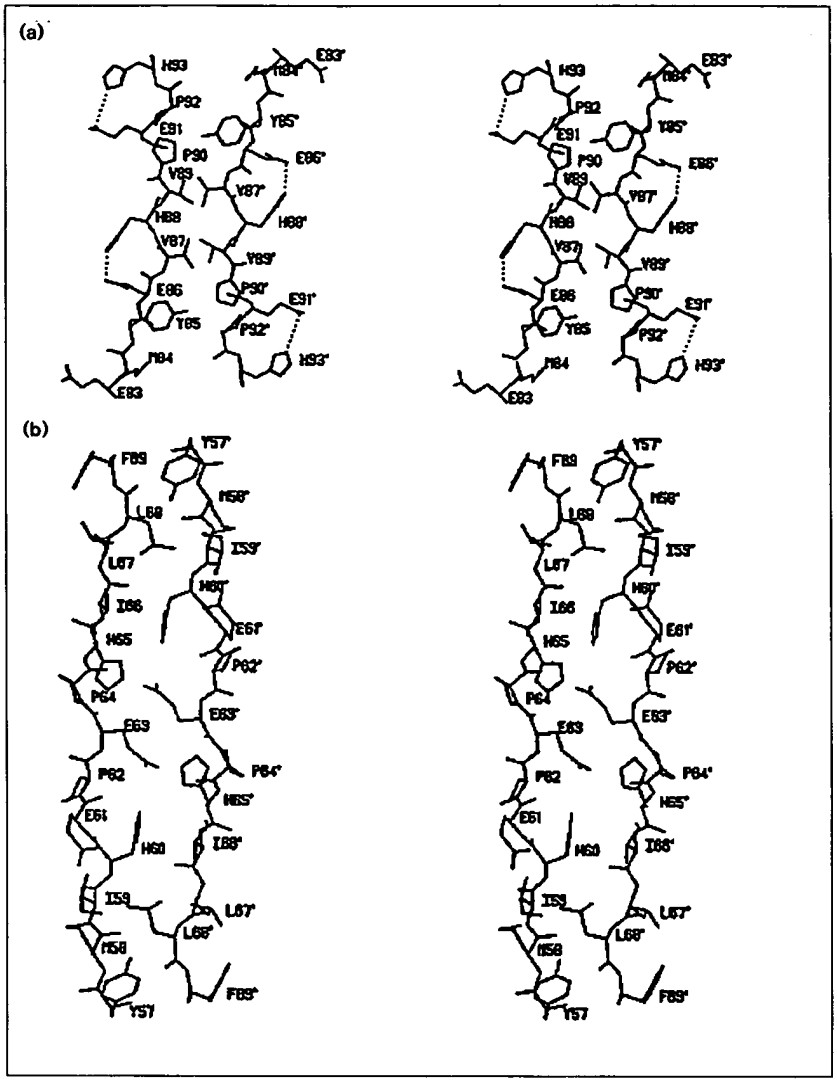

determined dimers (Table 3). The twist cannot be attributed to any specific residue. This is illustrated in Figure 5c. In fact, the conformational change is smoothly distributed through residues 85–92, which supports the idea that this region of the monomer represents a flexible hinge [22]. The p13or structure, however, does not reveal whether the inherent flexibility of this region allows the p13^{suc1} dimer to twist past the limits observed in the $P2_12_12_1$ structures.

A detailed view of the strand-exchange regions of the p13^{suc1} dimers is presented in Figure 5c. The monomers in the p13or dimer are related by crystallographic twofold symmetry and are therefore identical. In the previously determined dimers, however, no internal symmetry was present and the monomers comprising each dimer differed slightly. Overall, however, this region is very similar in the three dimers. Side chains for which the orientations are modelled differently, such as His88, are poorly defined in the electron density (Fig. 2b and [22]).

Finally, the prevalence of strand exchange in p13^{suc1} is confirmed by the observation of the dimer in two different space groups.

Comparison between the discrete monomer and the strand-exchanged dimer of p13^{suc1}

Figure 6 illustrates the dramatically different conformations adopted by residues 85–91 in the p13hex monomer relative to the p13or strand-exchanged dimer. The fact that the main-chain dihedral angles vary between p13or and p13hex throughout this region (Table 3), indicates that all of these residues contribute to the shape difference.

Figure 5

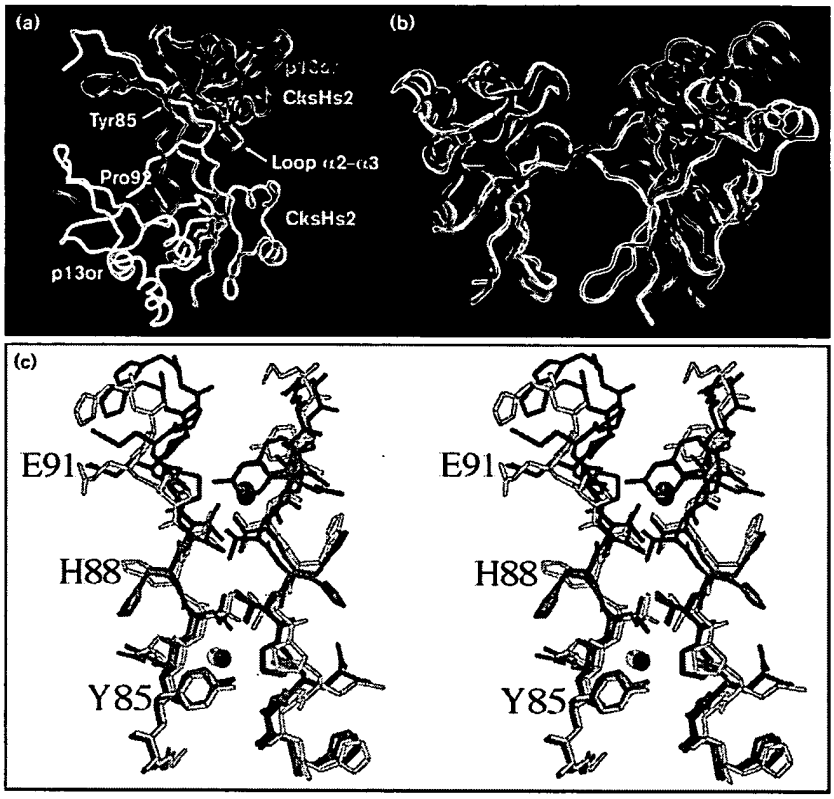

The strand-exchanged dimers. **(a)** Superposition of the CksHs2 monomer (magenta) [21] on the p13or monomer (red). Also shown are strand-exchange partners of both molecules (CksHs2, cyan and p13or, yellow). Arrows indicate residues in the strand-exchange region, Tyr85 and Pro92, which have significantly different ϕ and ψ angles in p13or and in CksHs2. The loop between α2 and α3, which is longer in $p13^{suc1}$ than in CksHs2, is also indicated. **(b)** Comparison of the $p13^{suc1}$ dimers with the left-hand monomer superimposed illustrates a twist in the dimer. The p13or dimer is shown in red. The two dimers in the asymmetric unit of the $P2_12_12_1$ structure [22] are shown in orange and magenta. **(c)** Superposition of the strand-exchange region of two $p13^{suc1}$ dimers from the $P2_12_12_1$ asymmetric unit (yellow and blue) with p13or (red). In p13or, two ordered water molecules, related by twofold symmetry, are present. Each dimer from the space group $P2_12_12_1$ has only one water molecule in this region. (Panels (a) and (b) generated with the program Raster3D [38]; panel (c) generated with MOLSCRIPT [37].)

In the discrete monomer, there are two prominent patches of conserved residues, one consisting of hydrophobic amino acids, and the other of positively charged amino acids (Fig. 7a). The hydrophobic patch contains residues Tyr31, Tyr36, Tyr38, His40, Met42, Tyr85, His88, Val89, Pro90, Pro92, Ile94 and Leu96. This patch is altered bystrand exchange in p13or (Fig. 7b). The hydrophobic surface of the monomer merges with that of its strand-exchange partner to yield an arch lined by hydrophobic residues. In the strand-exchanged dimer, the hydrophobic patch on each lobe is less accessible than in the p13hex monomer due to the proximity of the strand-exchange partner and the presence of a CHAPS molecule (Figs 1b,7b). Two symmetry-related CHAPS molecules are found within the arch. The O3 atom of each CHAPS molecule makes a hydrogen bond to the carbonyl oxygen

Table 3

Comparison of strand-exchange region of p13or with the corresponding regions of CksHs2, p13hex and the $p13^{suc1}$ dimers from space group $P2_12_12_1$ (p13′ and p13″).

Sequence		|p13or–CksHs2(C)|		|p13or–p13hex|		|p13or–p13′|		|p13or–p13″|	
$p13^{suc1}$	CksHs2	$\Delta\phi$ (°)	$\Delta\psi$ (°)	$\Delta\phi$ (°)	$\Delta\psi$ (°)	$\Delta\phi$ (°)	$\Delta\psi$ (°)	$\Delta\phi$ (°)	$\Delta\psi$ (°)
Tyr85	Tyr57	48	175	46	172	1	0	34	6
Glu86	Met58	24	22	95	18	8	7	10	21
Val87	Ile59	7	8	16	6	22	41	18	3
His88	His60	37	39	24	138	20	29	16	18
Val89	Glu61	38	28	61	170	20	3	7	13
Pro90	Pro62	14	4	16	145	20	22	13	26
Glu91	Glu63	26	23	86	84	6	9	0	13
Pro92	Pro64	4	177	13	9	8	12	12	4

The absolute values of differences in main-chain dihedral angles are shown.

Figure 6

Comparison of the strand-exchange region of p13or with the corresponding loop in p13hex. Residues in p13or and in its strand-exchange partner are shown in grey and white, respectively. The corresponding loop in p13hex is shown in black. (This figure was generated using MOLSCRIPT [37].)

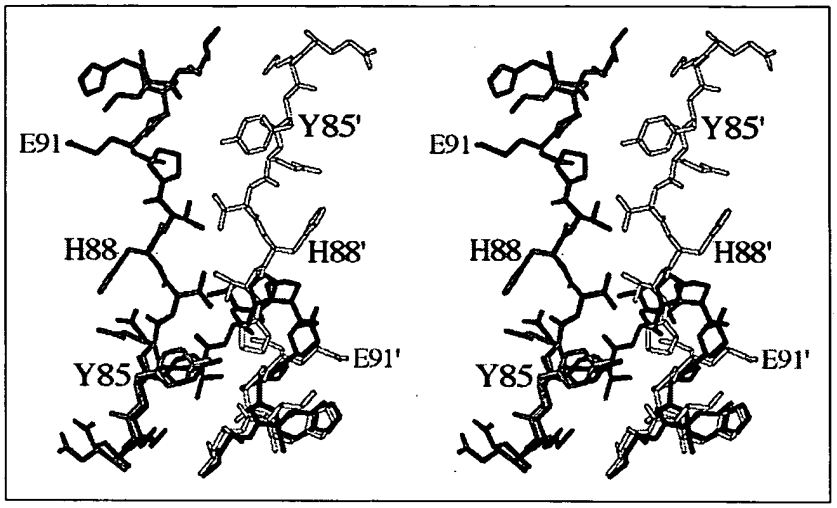

of His88 and there are several van der Waals contacts within 4 Å observed between the detergent and residues in the hydrophobic patch (Tyr31, His40, Tyr85, Val87, His88′, Pro90′ and Leu96′). The lack of electron density for the aliphatic tails of the detergent molecules suggest that they are probably quite mobile. It is possible that CHAPS mimics a hydrophobic patch on p34^{cdc2} kinase that serves as the binding site for p13^{suc1}. Alternatively, the detergent may represent a biologically relevant lipid or phospholipid, which could imply a connection between the control of multimeric assembly of p13^{suc1} and the phospholipid membrane.

The second conserved region, a patch of positively charged residues (Arg30, Arg39 and Arg99), has been shown to bind a sulphate anion in the CksHs2 crystal, and is proposed to be the potential binding site for phosphate on the target protein [4,21]. The same cluster is found in the p13or structure, but Arg99 originates from the strand-exchange partner. A chloride ion is bound to this site in the previously determined p13^{suc1} strand-exchanged dimer [22]. In p13or, the positive charges are partially balanced by Glu16 and Glu19 of a symmetry-related molecule, rather than by an external anion. This electrostatic interaction with a symmetry-related molecule is similar to the one observed in p13hex. The fact that a potential binding site for a phosphate group on CDK has been preserved intact in the strand-exchanged dimer, suggests that the dimerization of p13^{suc1} mediated by strand exchange results in aggregation of the CDK. This idea has been proposed by Parge *et al.* in regard to CksHs2 [21].

In the structure of p13hex, the asymmetric unit contained two molecules held together by the coordination of two zinc ions and by a network of electrostatic protein–protein interactions. In the case of p13hex, zinc had been included in crystallization trials, based on the observation that this metal caused dimerization of p13^{suc1} in solution

Figure 7

Comparison of conserved surface patches in p13or and p13hex. The conserved hydrophobic patch is shown in orange, and the positively charged patch in purple for **(a)** p13hex [19] and **(b)** p13or. The CHAPS molecule is shown in green with the oxygen atoms in red. The molecular symmetry twofold axis is vertical in this view. (Figure generated with the program GRASP [39].)

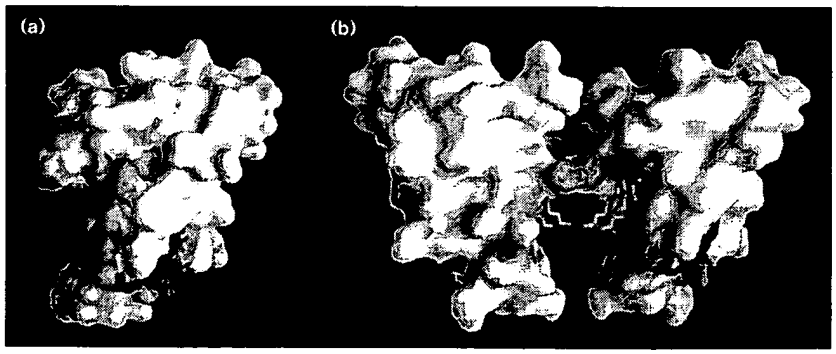

[19]. Zinc was not used in the crystallization of p13or, and the assembly observed in the p13or crystal is a strand-exchanged dimer. A monomer interface similar to the one found in the p13hex asymmetric unit is also present in the p13or crystal. The interface is on the side of the molecule opposite to that where strand exchange occurs, and results from crystal packing around a twofold axis (Fig. 8). Thirty water molecules are present at this interface in p13or. The two monomers in the orthorhombic crystal are farther apart than in the hexagonal system and consequently the electrostatic interactions between them should be weaker.

The p13or and p13hex [19] structures are interesting from a protein folding perspective. The identical sequence (YEVHVPEP, 85–92) adopts two very different conformations in the monomer and the strand-exchanged dimer. The result of changing the conformation of these eight residues is minimized by effectively keeping the environment of the residues preceding and following them constant. The exchanged β-strand (β4) makes the same contacts in the dimer as in the monomer. Therefore, the conformation of the segment from Tyr85–Pro92 is determined not only by its sequence, but also by the sequences of residues surrounding it. Questions consequently arise regarding the dynamics of the strand-exchange event. What triggers the monomer–dimer switch? How does the exchange take place? Does dimer association precede strand release from the monomer? Does the β-strand unthread from its sheet, or does it snap out in a 'mousetrap' mechanism, as proposed by Arvai *et al.* for CksHs1 [20]? Further biochemical and theoretical studies on the suc1/CKS system should help to clarify these points.

Figure 8

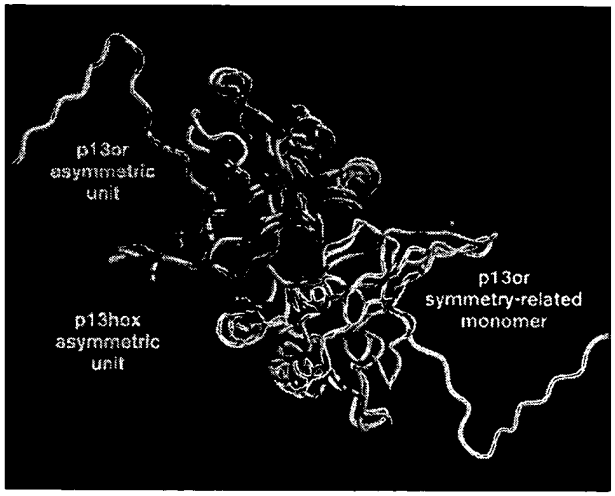

Superposition of p13hex and p13or. The asymmetric unit of p13or (red) is superimposed on subunit A of p13hex (blue) [19]. Also shown is a symmetry-related monomer of p13or (green), which illustrates that a similar interface exists in both crystal forms. (Figure generated with the program Raster3D [38].)

Strand exchange in $p13^{suc1}$ may be considered a domain-swapping phenomenon, a number of which have recently been described in the literature [24]. For instance, bovine seminal ribonuclease forms a dimer by exchanging N-terminal α-helices [25]. Similarly, a mutant of staphylococcal nuclease has been shown to dimerize by swapping C-terminal α-helices [26]. The cytokine, interleukin-5, exchanges a C-terminal strand and helix between monomers [27]. Other examples are βB2-crystallin [28] and diphtheria toxin [29], which swap entire domains to achieve dimerization. Clearly, domain swapping is an efficient way of forming a tightly associated dimer. It will be interesting to see if any other biological systems adopt this means of assembly, and how domain-swapping affects their function.

The process of strand exchange may also be compared with the conformational change proposed to be the basis of the inhibitory activity of serpins. In the serpins, a segment of polypeptide is believed to undergo a large movement and insertion into a β-sheet [30], similar to the latter part of strand exchange in $p13^{suc1}$.

Biological implications

The *C*DC28 *k*inase *s*pecific (CKS) cell-cycle control proteins regulate specific cyclin-dependent kinases (CDKs). Although the exact mechanism of action of the CKS proteins is not yet clear, it is believed to involve binding to the target CDK. This interaction may be dependent on the oligomeric state of the CKS protein. An understanding of the oligomerization properties of the CKS proteins is therefore crucial to the elucidation of their function.

The *Schizosaccharomyces pombe* protein, $p13^{suc1}$, a member of the CKS family, has been found in two conformations, the monomer and the strand-exchanged dimer. Two different oligomeric assemblies, a monomer and hexamer consisting of three strand-exchanged dimers, have also been observed for its closely related human homologues, CksHs1 and CksHs2, respectively [20,21]. In addition, hydrodynamic studies have shown that different multimeric states are possible for these proteins [20,21]. These results suggest that the switch between a monomer and a strand-exchanged assembly may govern the function of $p13^{suc1}$ perhaps by controlling the multimeric state of the protein or the integrity of the conserved surface patches. Finally, each form of the protein may possess different functional properties, which may account for the apparent paradox that $p13^{suc1}$ inhibits its wild-type target, $p34^{cdc2}$, but rescues a temperature-sensitive mutant of this same kinase.

Materials and methods

Materials

The Mono Q FPLC column and Sepharose CL6B were obtained from Pharmacia (Uppsala, Sweden). Bio-Gel hydroxyapatite beads were from Bio-Rad (Hercules, CA). Benzamidine, phenylmethylsulfonyl fluoride (PMSF), (*N*-[*N*-(L-3-*trans*-carboxyoxirane-2-carbonyl)-L-leucyl]-agmatine, aprotinin, leupeptin, pepstatin, L-1-chloro-3-(4-tosylamido)-7-amino-2-heptanone hydrochloride, L-1-chloro-3-(4-tosylamido)-4-phenyl-2-butanone, (4-amidinophenyl)-methansulfonyl flouride, phosphoramidon, dithiothreitol, isopropyl-β-D-thiogalactoside (IPTG) and dimethyl-sulfoxide (DMSO) were obtained from Boehringer Mannheim (Indianapolis, IN). 3-[(3-Cholamidopropyl)dimethylammonio]-1-propanesulfonate hydrate (CHAPS) was obtained from Sigma (St. Louis, MO) and polyethylene glycol 2000 monomethyl ether (PEG MME 2000) was from Fluka (Ronkonkoma, NY). The BL21(DE3) *Escherichia coli* host containing the p13^{suc1} expression vector was a generous gift of Dr J Wang, University of Calgary. All chemicals were of the highest grade available.

Expression and isolation of recombinant p13^{suc1}

Modified procedure of Brizuela *et al.* [5] was used for purification of the p13^{suc1} used for the crystallographic studies. An overnight culture of BL21(DE3) cells containing the p13^{suc1} expression vector was transferred to fresh medium (Luria broth containing ampicillin at 50 μg ml^{-1}), and grown to mid-log phase (OD_{600}=0.6–1.0) followed by the induction of the expression of the fusion protein for 3.5 h with 0.1 mM IPTG. Cells were spun down at 3500*g* for 20 min and the pellet was resuspended in 1 mM EDTA and 50 mM Tris, pH 7.0 in the presence of a mixture of the following proteinase inhibitors made in 2000 times stock solution in 50% (v/v) DMSO: 0.5 mM benzamidine, 0.5 mM PMSF, 0.5 μg ml^{-1} of (*N*-[*N*-(L-3-*trans*-carboxyoxirane-2-carbonyl)-L-leucyl]-agmatine, 0.1 μg ml^{-1} of aprotinin, 0.5 μg ml^{-1} of leupeptin, 0.5 μg ml^{-1} of pepstatin, 50 μg ml^{-1} each of L-1-chloro-3-(4-tosylamido)-7-amino-2-heptanone hydrochloride and L-1-chloro-3-(4-tosylamido)-4-phenyl-2-butanone, 0.1 μg ml^{-1} of (4-amidinophenyl)-methansulfonyl fluoride, 50 μg ml^{-1} of phosphoramidon. Cells were lysed by passage through a French Press set at 1000 psi. The extract was centrifuged at 10000*g* for 10 min and the supernatant (containing the fusion protein) was then assayed for protein content. The soluble fraction was loaded on a 1.5×80 cm Sepharose CL6B column and eluted with 1 mM EDTA and 50 mM Tris, pH 7.0 at a flow rate of 0.3 ml min^{-1}. Fractions of 3 ml volume were collected and analyzed by SDS-PAGE. Fractions containing p13^{suc1} were dialyzed for 18 h against a buffer containing 50 mM Tris, pH 7.0. The dialyzed sample was applied directly onto a Mono Q FPLC column that had been washed with three column volumes of 50 mM Tris, pH 8.0. Elution was carried out with a salt gradient (0–300 mM NaCl) in 50 mM Tris, pH 8.0 at a rate of 1 ml min^{-1}. Fractions of 1 ml volume were collected and analyzed by SDS-PAGE. Samples containing p13^{suc1} were again loaded on a Sepharose CL6B column equilibrated with 50 mM Tris, pH 7.0. Fractions of 3 ml volume were collected followed by dialysis for 16 h against 10 mM potassium phosphate, pH 7.0. Further purification of p13^{suc1} was achieved by hydroxyapatite chromatography. The sample was loaded onto a hydroxyapatite column (2 cm×15 cm; flow rate 0.5 ml min^{-1} and unbound protein was washed out with 150 ml of 10 mM potassium phosphate, pH 7.0. The bound proteins were eluted with a 400 ml linear gradient of 10 mM to 1000 mM potassium phosphate, pH 7.0. Fractions of 5 ml volume were collected and analyzed for the presence of p13^{suc1} by SDS-PAGE.

N-terminal sequencing revealed that the N-terminal methionine had been removed and that the recombinant p13^{suc1} starts at Ser2. Electrospray mass spectrometry confirmed that this protein contained 105 residues (2–106). Four residues at the C terminus (107–113) had been removed during protein expression.

Crystallization and data collection

p13^{suc1} was crystallized in space group $C222_1$, a=43.27 Å, b=55.28 Å, c=111.80 Å, with one molecule in the asymmetric unit. Crystals were grown at room temperature by the vapour diffusion method. Sitting drops of 8 μl containing recombinant p13^{suc1} [12 mg ml^{-1} in 38 mM LiCl, 38 mM Tris (pH 7.8), 9% (w/v) PEG MME 2000 and 0.4% (w/v) CHAPS] were equilibrated with 1 ml of 25%

Figure 9

Electron density for CHAPS. $2F_o-F_c$, 1σ electron density and the CHAPS molecule from the current model. Only the first four carbons of the detergent tail are defined in the electron-density map. The complete structure of the detergent tail is $-C^{20}(CH_3)(CH_2)_2CONH(CH_2)_3N^+(CH_3)_2(CH_2)_3SO_3^-$.

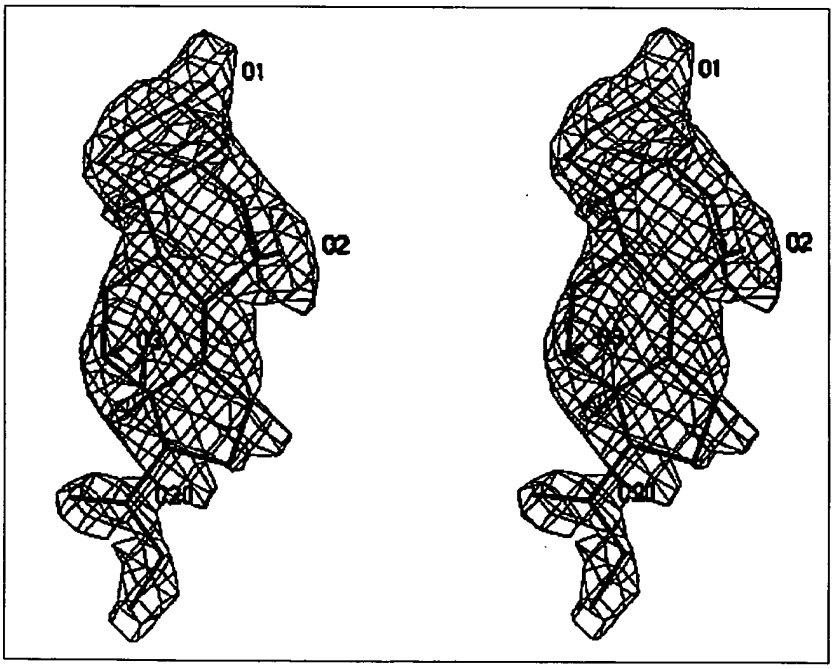

PEG MME 2000, 0.1 M LiCl, 0.1 M Tris (pH 7.8). CHAPS was found to improve crystal quality. Seeding was used to obtain crystals suitable for data collection. X-ray diffraction data for a single crystal of $p13^{suc1}$ were collected at room temperature on a San Diego Multiwire Systems area detector to 1.95 Å (Table 1). Graphite monochromated CuKα radiation was generated with a Rigaku rotating anode generator RU-200 BH operating at 40 kV and 150 mA.

Structure determination and refinement

The p13or structure was solved by molecular replacement using the AMoRe [31] package. Monomer A of the p13hex structure [19], residues 6–101, was used as the search model. Rotation and translation, followed by rigid-body refinement, produced a clear solution with a correlation of 0.63 and an R-factor ($= \Sigma||F_o|-|F_c||/\Sigma|F_o|$) of 41%. This model was then subjected to energy minimization and molecular dynamics in X-PLOR [32]. At this stage the electron-density map was examined in O [33] and revealed a poorly defined loop structure for residues 86–92. These residues, and residues 6 and 7, were excluded from further refinement with TNT [34], and were gradually built into the electron density to yield the strand-exchange model (Fig. 2a,b). Alternating cycles of TNT refinement with manual refitting, yielded a model which included residues 5–102, and 37 water molecules. The R-factor of this model was 21.0%, and the free R-factor [35] was 29.3% for all data between 20 Å and 1.95 Å. At this point the electron-density map contained two features in the vicinity of the strand-exchange region that could not be assigned. The model was subjected to simulated annealing, energy minimization and B-factor refinement in X-PLOR [32]. The resulting electron-density map was sufficiently improved to allow the placement of the steroid nucleus of CHAPS, the detergent used in the crystallization, into one of the previously unassigned peaks (Fig. 9), as well as the addition of residues 2, 3 and 4 to the model. After several more rounds of energy minimization and B-factor refinement in X-PLOR, 45 more water molecules were added. The final model contains residues 2–102, 72 water molecules, and one CHAPS molecule per asymmetric unit. The final R-factor is 18.7%, and the free R-factor is 24.1% for all data between 6.0 and 1.95 Å (Table 1).

The atomic coordinates have been deposited in the Brookhaven protein data bank [36] (entry ID PUC1).

Acknowledgements

We would like to thank Louise Johnson for making p13hex coordinates available to us prior to publication. We thank Yves Bourne and John Tainer for providing the suc1 coordinates prior to release in the PDB. We also thank members of the James lab and RJ Read for helpful discussions. NK and KSB acknowledge NSERC and the Alberta Heritage Scholarship Fund, respectively, for predoctoral fellowships.

References

1. Hayles, J., Aves, S. & Nurse, P. (1986). *suc1* is an essential gene involved in both the cell cycle and growth in fission yeast. *EMBO J.* **5**, 3373–3379.
2. Hindley, J., Phear, G., Stein, M. & Beach, D. (1987). *Suc1*$^+$ encodes a predicted 13-kilodalton protein that is essential for cell viability and is directly involved in the division cycle of *Schizosaccharomyces pombe*. *Mol. Cell. Biol.* **7**, 504–511.
3. Moreno, S., Hayles, J. & Nurse, P. (1989). Regulation of $p34^{cdc2}$ protein kinase during mitosis. *Cell* **58**, 361–372.
4. Endicott, J.A. & Nurse, P. (1995). The cell cycle and suc1: from structure to function? *Structure* **3**, 321–325.
5. Brizuela, L., Draetta, G. & Beach, D. (1987). $p13^{suc1}$ acts in the fission yeast cell division cycle as a component of the $p34^{cdc2}$ protein kinase. *EMBO J.* **6**, 3507–3514.
6. Forsburg, S.L. & Nurse, P. (1991). Cell cycle regulation in the yeasts *Saccharomyces cerevisiae* and *Schizosaccharomyces pombe*. *Annu. Rev. Cell Biol.* **7**, 227–256.
7. Nurse, P. & Bissett, Y. (1981). Gene required in G1 for commitment to cell cycle and in G2 for control of mitosis in fission yeast. *Nature* **292**, 558–560.
8. Surana, U., Robitsch, H., Price, C., Schuster, T., Fitch, I. & Futcher, A.B. (1991). The role of CDC28 and cyclins during mitosis in the budding yeast *S. cerevisiae*. *Cell* **65**, 145–161.
9. Simani, V. & Nurse, P. (1986). The cell cycle control gene *cdc2*$^+$ of fission yeast encodes a protein kinase potentially regulated by phosphorylation. *Cell* **45**, 261–268.
10. Dunphy, W.G. (1994). The decision to enter mitosis. *Trends Cell. Biol.* **4**, 202–207.
11. Solomon, M.J. (1993). Activation of the various cyclin/cdc2 protein kinases. *Curr. Opin. Cell Biol.* **5**, 180–186.
12. Hayles, J., Beach, D., Durkacz, B. & Nurse, P. (1986). The fission yeast cell cycle control gene *cdc2*; isolation of a sequence *suc1*, that suppresses *cdc2* mutant function. *Mol. Gen. Genet.* **202**, 291–293.
13. Hadwiger, J.A., Wittenberg, C., Mendenhall, M.D. & Reed, S.I. (1989). The *Saccharomyces cerevisiae* CKS1 gene, a homolog of the *Schizosaccharomyces pombe suc1*$^+$ gene, encodes a subunit of the cdc28 protein kinase complex. *Mol. Cell. Biol.* **9**, 2034–2041.
14. John, P.C.L., Sek, F.J. & Hayles, J. (1991). Association of the plant $p34^{cdc2}$-like protein with $p13^{suc1}$: implications for control of cell division cycle in plants. *Protoplasma* **161**, 70–74.
15. Hepler, P.K., Sek, F.J. & John, P.C.L. (1994). Nuclear concentration and mitotic dispersion of the essential cell cycle protein, $p13^{suc1}$, examined in living cells. *Proc. Natl. Acad. Sci. USA* **91**, 2176–2180.
16. Colas, P., Serras, F. & Van Loon, A.E. (1993). Microinjection of suc1 transcripts delays the cell cycle clock in *Patella vulgata* embryos. *Int. J. Dev. Biol.* **37**, 589–94.
17. Dunphy, W.G. & Newport, J.W. (1989). Fission yeast p13 blocks mitotic activation and tyrosine dephosphorylation of the *Xenopus* cdc2 protein kinase. *Cell* **58**, 181–191.
18. Kusubata, M., *et al.*, & Inagaki, M. (1992). $p13^{suc1}$ suppresses the catalytic function of $p34^{cdc2}$ kinase for intermediate filament proteins, *in vitro*. *J. Biol. Chem.* **267**, 20937–20942.
19. Endicott, J.A., *et al.*, & Johnson, L.N. (1995). The crystal structure of $p13^{suc1}$, a $p34^{cdc2}$-interacting cell cycle control protein. *EMBO J.* **14**, 1004–1014.
20. Arvai, A.S., Bourne, Y., Hickey, M.J. & Tainer, J.A. (1995). Crystal structure of the human cell cycle protein CksHs1: single domain fold with similarity to kinase N-lobe domain. *J. Mol. Biol.* **249**, 835–842.
21. Parge, H.E., Arvai, A.S., Murtari, D.J., Reed, S.I. & Tainer, J.A. (1993). Human CksHs2 atomic structure: a role for its hexameric assembly in cell cycle control. *Science* **262**, 387–395.
22. Bourne, Y., *et al.*, & Tainer, J.A. (1995). Crystal structure of the cell cycle-regulatory protein suc1 reveals a β-hinge conformational switch. *Proc. Natl. Acad. Sci. USA* **92**, 10232–10236.
23. Laskowski, R.A., MacArthur, M.W., Moss, D.S. & Thornton, J.M. (1993). PROCHECK: a program to check the stereochemical quality of protein structures. *J. Appl. Cryst.* **26**, 283–291.
24. Bennett, M.J., Schlunegger, M.P. & Eisenberg, D. (1995). 3D domain swapping: a mechanism for oligomer assembly. *Protein Sci.* **4**, 2455–2468.
25. Mazzarella, L., *et al.*, & Zagari, A. (1993). Bovine seminal ribonuclease: Structure at 1.9 Å resolution. *Acta Cryst. D* **49**, 389–402.
26. Green, S.M., Gittis, A.G., Meeker, A.K. & Lattman, E.E. (1995). One-step evolution of a dimer from a monomeric protein. *Nature Struct. Biol.* **2**, 746–751.
27. Milburn, M.V., *et al.*, & Wells, T.N.C. (1993). A novel dimer configuration revealed by the crystal structure at 2.4 Å resolution of human interleukin-5. *Nature* **363**, 172–176.
28. Lapatto, R., *et al.*, & Slingsby C. (1991). High resolution structure of an oligomeric eye lens beta-crystallin. Loops, arches, linkers and interfaces in beta B2 dimer compared to a monomeric gamma-crystallin. *J. Mol. Biol.* **222**, 1067–1083.
29. Bennett, M.J., Choe, S. & Eisenberg, D. (1994). Domain swapping: entangling alliances between proteins. *Proc. Natl. Acad. Sci. USA* **91**, 3127–3131.
30. Carrell, R.W. & Evans, D.L.I. (1992). Serpins: mobile conformations in a family of proteinase inhibitors. *Curr. Opin. Struct. Biol.* **2**, 438–446.
31. Navaza, J. (1994). AMoRe: an automated package for molecular replacement. *Acta Cryst. A* **50**, 157–163.
32. Brünger, A.T. (1993). *X-PLOR: A System for X-ray Crystallography and NMR*. Yale University Press, New Haven, CT.
33. Jones, T.A., Zou, J.Y., Cowan, S.W. & Kjeldgaard, M. (1991). Improved methods for building protein models in electron density maps and the location of errors in these models. *Acta Cryst. A* **47**, 110–119.
34. Tronrud, D.E. (1992). Conjugate-direction minimization: an improved method for the refinement of macromolecules. *Acta Cryst. A* **48**, 912–916.

35. Brünger, A.T. (1992). Free R value: a novel statistical quantity for assessing the accuracy of crystal structures. *Nature* **355**, 472–475.
36. Bernstein, F.C., *et al.*, & Tasumi, M. (1977). The protein data bank: a computer based archival file for macromolecular structures. *J. Mol. Biol.* **112**, 535–542.
37. Kraulis, P.J. (1991). MOLSCRIPT: a program to produce both detailed and schematic plots of protein structures. *J. Appl. Cryst.* **24**, 946–950.
38. Bacon, D.J. & Anderson, W.F. (1988). A fast algorithm for rendering space-filling molecule pictures. *J. Mol. Graphics* **6**, 219–220.
39. Nicholls, A., Sharp, K. & Honig, B. (1991). Protein folding and association: insights from the interfacial and thermodynamic properties of hydrocarbons. *Proteins* **11**, 281–296.